Determination of the $N = 16$ Shell Closure at the Oxygen Drip Line

C. R. Hoffman,[1,*] T. Baumann,[2] D. Bazin,[2] J. Brown,[3] G. Christian,[2,4] P. A. DeYoung,[5] J. E. Finck,[6] N. Frank,[2,4,†] J. Hinnefeld,[7] R. Howes,[8] P. Mears,[5] E. Mosby,[9] S. Mosby,[9] J. Reith,[5] B. Rizzo,[8] W. F. Rogers,[9] G. Peaslee,[5] W. A. Peters,[2,4,‡] A. Schiller,[2,§] M. J. Scott,[6] S. L. Tabor,[1] M. Thoennessen,[2,4] P. J. Voss,[6] and T. Williams[3]

[1]*Department of Physics, Florida State University, Tallahassee, Florida 32303, USA*
[2]*National Superconducting Cyclotron Laboratory, Michigan State University, East Lansing, Michigan 48824, USA*
[3]*Department of Physics, Wabash College, Crawfordsville, Indiana 47933, USA*
[4]*Department of Physics & Astronomy, Michigan State University, East Lansing, Michigan 48824, USA*
[5]*Department of Physics, Hope College, Holland, Michigan 49423, USA*
[6]*Department of Physics, Central Michigan University, Mt. Pleasant, Michigan, 48859, USA*
[7]*Department of Physics & Astronomy, Indiana University at South Bend, South Bend, Indiana 46634, USA*
[8]*Department of Physics, Marquette University, Milwaukee, Wisconsin 53201, USA*
[9]*Department of Physics, Westmont College, Santa Barbara, California 93108, USA*

(Received 22 December 2007; published 17 April 2008)

The neutron unbound ground state of ^{25}O ($Z = 8$, $N = 17$) was observed for the first time in a proton knockout reaction from a ^{26}F beam. A single resonance was found in the invariant mass spectrum corresponding to a neutron decay energy of 770^{+20}_{-10} keV with a total width of 172(30) keV. The $N = 16$ shell gap was established to be 4.86(13) MeV by the energy difference between the $\nu 1s_{1/2}$ and $\nu 0d_{3/2}$ orbitals. The neutron separation energies for ^{25}O agree with the calculations of the universal *sd* shell model interaction. This interaction incorrectly predicts an ^{26}O ground state that is bound to two-neutron decay by 1 MeV, leading to a discrepancy between the theoretical calculations and experiment as to the particle stability of ^{26}O. The observed decay width was found to be on the order of a factor of 2 larger than the calculated single-particle width using a Woods-Saxon potential.

DOI: 10.1103/PhysRevLett.100.152502 PACS numbers: 21.10.Pc, 25.60.−t, 27.30.+t, 29.30.Hs

The determination of the limit of nuclear stability is one of the fundamental questions in nuclear physics. The location of the neutron drip line is only known for the lightest isotopes, and the recent discovery of ^{40}Mg and ^{42}Al demonstrates that the nuclear force is not well understood for neutron-rich nuclei [1]. One continuing puzzle exists in the mass $A = 20$–30 region where, experimentally, the oxygen isotopes are known to have an abrupt end at ^{24}O ($N = 16$) [2–5], while the fluorine ($Z = 9$) isotopes extend to at least ^{31}F ($N = 22$) [6]. This sudden change in the nuclear binding is believed to be the result of an increased shell gap, defined as the energy difference between the $\nu 1s_{1/2}$ and $\nu 0d_{3/2}$ single-particle levels, at neutron number 16 ($N = 16$) [7]. The relatively large energy difference between the single-particle orbitals results in a new shell closure (magic number) at $N = 16$ for the neutron-rich oxygen isotopes. The emergence of this new magic number has been attributed to the presence of a neutron skin or halo [8] and the tensor force [9,10].

Although some evidence for the $N = 16$ shell gap has been reported [8,11,12], a direct measurement of the $\nu 0d_{3/2}$ single-particle energy at the oxygen drip line had not been performed. A measurement of this orbital determines the ground state binding energy of ^{25}O, the first oxygen isotope beyond the neutron drip line, along with the size of the $N = 16$ shell closure. Theoretical predictions of the stability of the next even-even oxygen isotope (^{26}O) have differed considerably [13–17]. The universal *sd* (USD) [13] shell model interaction and the finite range droplet model [16] (FRDM) both predict an ^{26}O ground state that is bound to two-neutron decay; however, strong experimental evidence suggests that it does not exist [2,3]. The Hartree-Fock-Bogoliubov (HFB-8) model [17] and the USD05a [15] interaction both reproduce the oxygen drip line correctly, but the HFB-8 model, in particular, drastically underestimates the last bound fluorine isotope to be ^{27}F ($N = 18$). Therefore, a mass measurement of ^{25}O adds significant constraints on the theoretical calculations for the binding of ^{26}O.

In this Letter we report on the first mass measurement of ^{25}O, populated in a one-proton stripping reaction from a secondary ^{26}F beam. Invariant mass spectroscopy is used to reconstruct the unbound ^{25}O ground state on an event-by-event basis from a full momentum measurement of the neutron and the ^{24}O fragment. This is the first time this technique has been employed for such a heavy isotope beyond the neutron drip line. Until the present work, ^{16}B was the heaviest neutron unbound ground state for which spectroscopic information was available [18].

An 85 MeV/u secondary beam of ^{26}F was produced at the National Superconducting Cyclotron Laboratory (NSCL) at Michigan State University from the fragmenta-

tion of a 140 MeV/u $^{48}Ca^{20+}$ primary beam on a 987 mg/cm^2 Be production target. The A1900 fragment separator [19] was optimized for the isotopic selection of ^{26}F and utilized a 1050 mg/cm^2 Al wedge that was located at its intermediate focal plane. The momentum acceptance was limited to $\Delta p/p = 2\%$ and a secondary beam purity of 50% was achieved. The ^{26}F beam was identified event by event by its time of flight, and was focused on a 470 mg/cm^2 Be reaction target at a rate of ~20 pps.

The charged fragments exiting the target were deflected by the large-gap Sweeper magnet [20], and were recorded by position and energy sensitive detectors. A novel partial inverse matrix technique [21] was used to reconstruct the momenta of the ^{24}O fragments at the point of breakup. Neutrons were detected around 0° with the Modular Neutron Array (MoNA) [22]. Further details about the experimental setup and analysis procedures are described in Ref. [23].

The mass of ^{25}O was calculated from the fragment (E_f) and neutron (E_n) total energies, corresponding momenta (p_f, p_n) and their relative opening angle (Θ) according to

$$M = \sqrt{m_f^2 + m_n^2 + 2(E_f E_n - p_f p_n \cos\Theta)} \qquad (1)$$

where m_f and m_n are the ^{24}O and neutron rest masses. The measured kinetic energies for coincidence ^{24}O fragments and neutrons are shown by the data points in Figs. 1(a) and 1(b), along with the reconstructed opening angle (in the lab frame) between the ^{24}O-n pairs [Fig. 1(c)]. The final energy and angle resolutions of the ^{24}O fragments were 0.84 MeV/u and 7.2 mrad FWHM, respectively. Neutrons emanating from the ^{25}O decays were reconstructed with 4.2 MeV FWHM energy resolution and 19.4 mrad FWHM angular resolutions.

The neutron decay energy is directly related to the mass via $E_{\rm decay} = M - m_f - m_n$, and is shown by the data points in Fig. 2. A single resonance was observed and a Monte Carlo simulation was carried out to extract the decay energy and width. The simulation accounted for the geometric acceptances of the neutrons and fragments as well as the detector responses. Angular straggling of fragments in the target and a Glauber reaction model were also included. The experimental resolution (FWHM) for the $^{25}\mathrm{O} \rightarrow {}^{24}\mathrm{O} + n$ decay was found to scale as $18\sqrt{E_{\rm decay}(\mathrm{keV})}$ and $40\sqrt{E_{\rm decay}(\mathrm{keV})} - 700(\mathrm{keV})$ below and above $E_{\rm decay} \sim 1$ MeV, respectively.

The distribution of the neutron decay was simulated with a single resonance in addition to a nonresonance contribution of beam velocity neutrons with a Maxwellian distribution. The resonance was described by a single-level Breit-Wigner line shape as given by the prescription in Ref. [24]. The energy dependent width, $\Gamma = 2P_l(E)\gamma^2$, where γ is the reduced width and $P_l(E)$ is the penetrability function, represents the total decay width when evaluated at the resonant energy ($E_{\rm decay}$). The distribution was found to be insensitive to the size of the channel radius (a between 5.44 and 5.83 fm). The energy shift (Δ) can be expressed in terms of the shift function ($S_l(E)$) and the boundary condition parameter (B), $\Delta = -(S_l(E) - B)\gamma^2$.

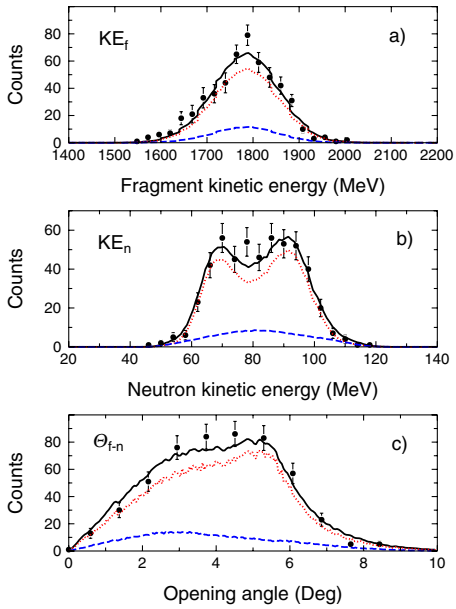

FIG. 1 (color online). Measured ^{24}O fragment kinetic energies (a), neutron kinetic energies (b), and their relative decay angle (c) are shown by the data points with their statistical errors. The results of Monte Carlo simulation are shown by the solid black lines which are comprised of the sum of the resonant (red, dotted) and nonresonant (blue, dashed) contributions to the decay spectrum (see text).

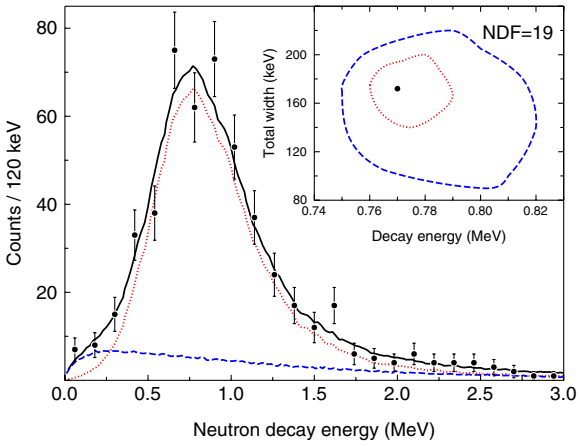

FIG. 2 (color online). The reconstructed neutron decay energy spectrum of ^{25}O is shown by the data points. The solid black line shows the simulated line-shape composed of a resonant (red, dotted) ($E_{\rm decay} = 770$ keV, $\Gamma = 172$ keV, $l = 2$) and nonresonant (blue, dashed) contribution (ratio 3.25:1). The inset shows a contour plot of the χ^2 dependence ($N = 19$ degrees of freedom) of the Breit-Wigner parameters for decay energy ($E_{\rm decay}$) and total width (Γ). The red (dotted) and blue (dashed) contours represent the 1 and 2 σ limits, respectively.

The boundary condition was set so as to eliminate the shift energy at the resonant energy, i.e., $B = S_l(E_{\mathrm{decay}})$. An angular momentum value of $l = 2$ was used because the ground state of ^{25}O is predicted to be a $3/2^+$ state [13–15] decaying to the 0^+ ground state of ^{24}O.

The decay energy and total width were determined by a minimum χ^2 fitting to the decay spectrum. The resonant energy, partial width, energy of the Maxwellian distribution and the amplitudes of the resonant and nonresonant contributions were all free parameters of the fit. The simulations were convoluted with the experimental resolution to allow for a direct comparison with the experimental data. A resonance energy of $E_{\mathrm{decay}} = 770^{+20}_{-10}$ keV and a width of $\Gamma = 172(30)$ keV were the best fit to the data. The lines in Fig. 2 show the sum (black, solid) of the best fit, combining a resonance contribution (red, dotted) and a nonresonance background contribution (blue, dashed). The simulated data also reproduces all of the other experimental observables. The simulated fragment and neutron kinetic energies and the opening angle are shown as solid lines in Fig. 1.

The determination of the mass of ^{25}O from the resonance energy is dependent on the mass of ^{24}O. A recent experiment on neutron-rich nuclei remeasured the mass of ^{24}O, adopting a mass excess of 18600(100) keV [25], 470 keV below the currently accepted value of 19070(240) keV of the atomic mass evaluation (AME) [26]. The ^{25}O mass excess is then 27440(110) keV and 27910(245) keV for Ref. [25] and the AME, respectively. For all calculations and comparisons to theoretical results in this paper, the more recent measurement has been adopted.

The resonance energy can be used to determine the size of the $N = 16$ shell gap, given by the energy difference between the $\nu 1s_{1/2}$ and the $\nu 0d_{3/2}$ single-particle levels. Taking a closed-shell $(0p - 0h)$ configuration for the ^{24}O ground state, the $\nu 0d_{3/2}$ single-particle energy is the difference in binding energies between the ^{25}O and ^{24}O ground states (the observed decay energy), $\epsilon 0d_{3/2} = 770^{+20}_{-10}$ keV. The single-particle energy of the $\nu 1s_{1/2}$ orbital is given by the ^{24}O–^{23}O ground state's energy difference, $\epsilon 1s_{1/2} = -4.09(13)$ MeV. The single-particle energies for the two orbitals are plotted on the left-hand side of Fig. 3. The size of the $N = 16$ shell gap is then $\epsilon 0d_{3/2} - \epsilon 1s_{1/2} = 4.86(13)$ MeV. It should be noted that the use of the AME mass excess would reduce the $N = 16$ shell gap size to 4.39(25) MeV due to a change in the location of the $\nu 1s_{1/2}$ level ($\epsilon 1s_{1/2} = -3.62(25)$ MeV). The experimental $\nu 0d_{3/2}$ energy, however, is unaffected by the mass excess and as is described below, it is this orbital location that is most crucial to understanding the differences between the theoretical predictions and the oxygen drip line.

The experimental single-particle energies are compared to calculations using the USD [13], USD05a [15] and SDPF-M [14] shell model interactions and are shown as lines in Fig. 3. Compared to the original USD interaction, the USD05a interaction resulted from a more recent fit to experimental data, whereas the SDPF-M interaction includes the pf model space and an adjustment to the $0d_{5/2} - 0d_{3/2} T = 1$ two-body matrix element. While all three interactions agree on the energy of the $\nu 1s_{1/2}$ level, surprisingly only the original USD interaction reproduces the experimental $\nu 0d_{3/2}$ energy. The USD05a and SDPF-M interactions over-predict the location of the $\nu 0d_{3/2}$ level and thus the ^{25}O decay energy by $\sim$0.5 MeV and $\sim$1.2 MeV, respectively.

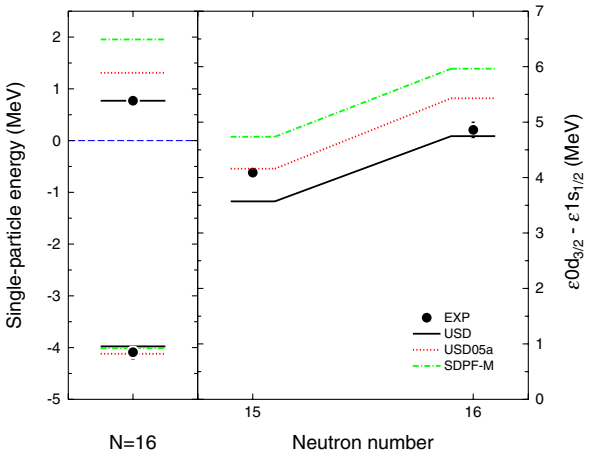

FIG. 3 (color online). The experimental (data points) and theoretical [13–15] (lines) single-particle energies (SPE) for the $\nu 1s_{1/2}$ and $\nu 0d_{3/2}$ orbitals at $N = 16$ are shown on the left. The difference between these SPEs is shown for $Z = 8$, $N = 15$ [12] and 16, giving the $N = 16$ shell gap size. Errors are shown if they are larger than the symbol size.

This observation is in contrast to the recent measurement of the $N = 16$ shell gap in ^{23}O which agreed with the calculation using the USD05a interaction [12]. In that work the $3/2^+$ energy level was found to be 4.00 MeV above the $1/2^+$ [27,28] ground state, giving the difference between the $\nu 1s_{1/2}$ and $\nu 0d_{3/2}$ orbitals. This value is compared to the measured shell gap at the drip line and the different shell model calculations on the right side of Fig. 3.

The energy of the $\nu 0d_{3/2}$ orbital is key to understanding the drip line since it is the main component in determining the binding energy of the ^{26}O ground state. To illustrate its effect, the one- and two-neutron separation energies are plotted for $^{23-26}$O in Fig. 4. The S_n and S_{2n} for ^{25}O are derived from the present result, and its ground state energy is sensitive to the $\nu 0d_{3/2}$ single-particle energy. The theoretical predictions using the USD, USD05a, and SDPF-M shell model interactions reproduce the experimental data up to the drip line; however, above this they diverge in their predictions of the ^{25,26}O neutron separation energies. The differences in the predicted separation energies of the three interactions for $N = 17$ and 18 are due mostly to the energy variation of the $\nu 0d_{3/2}$ single-particle level (see Fig. 3).

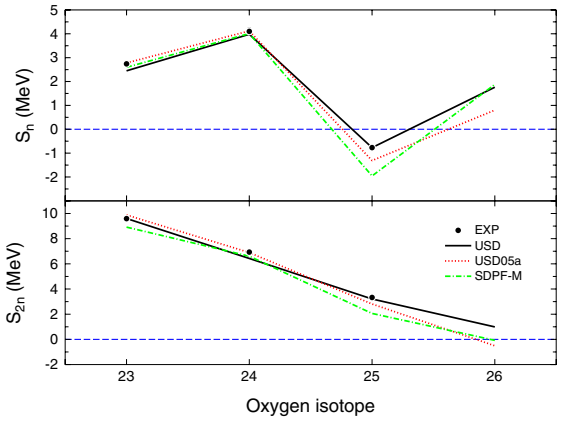

FIG. 4 (color online). The experimental [25,26] (data points) and theoretical [13–15] (lines) one- and two-neutron separation energies for the $N = 15$–18 oxygen isotopes. The experimental error is shown if it is larger than the symbol size.

As mentioned earlier, it is surprising that the original USD interaction reproduces the present measurement. Especially, because this interaction, if correct, predicts ^{26}O to be bound with respect to two-neutron decay by 1 MeV, which is inconsistent with the experimental observations [2,3]. The USD05a and SDPF-M interactions having $\nu 0d_{3/2}$ orbitals that lie higher in the continuum, result in predictions of a negative value for the S_{2n} of ^{26}O (-510 keV for the USD05a interaction and -77 keV for the SDPF-M interaction) in agreement with experiment [2,3]. The increased binding energy of ^{26}O for the SDPF-M comes from a small ($\sim 20\%$) $2p-2h$ excitation into the fp shell, which is not possible with the USD or USD05a interactions as they are confined to the sd single-particle space.

A possible cause for the reduction in the energy of the $\nu 0d_{3/2}$ orbital at the drip line could be correlations with the continuum. Although the two-body matrix elements for the aforementioned interactions do implicitly include resonance effects through their fitting to experimental data, the continuum is not explicitly handled. Current work is underway to directly include the unbound $\nu 0d_{3/2}$ orbital into shell model calculations for the neutron-rich oxygen isotopes [29].

The observed decay width (172(30) keV) is about a factor of 2 larger than the single-particle decay width of $\Gamma_{sp} = 79$ keV, calculated for the $l = 2$ ground state neutron decay of ^{25}O at 770 keV. The calculation was performed with a Woods-Saxon potential optimized by matching the single-particle states in ^{17}O ($5/2^+$, $1/2^+$ and $3/2^+$). The large decay width might be explained by the extended root-mean-square matter radius observed for the ground state of ^{24}O (3.19 ± 0.13 fm) [30]. Modifying a Woods-Saxon potential by increasing the diffuseness and/or radius to simulate the extended matter distribution, resulted in larger single-particle widths, consistent with the observed result. A neutron skin or halo [31,32] in the ground state of ^{24}O could present an explanation for the large matter distribution and hence the large decay width; however, determination of the proton (charge) distribution is needed.

In conclusion, the mass of ^{25}O has been measured for the first time. The size of the $N = 16$ shell gap was determined at the oxygen drip line, and a lowering of the $\nu 0d_{3/2}$ orbital was observed. The neutron separation energies for ^{25}O and the location of the oxygen drip line could not be simultaneously explained with either the USD, USD05a or SDPF-M shell model interactions, and the effects of the continuum must be investigated. The large decay width observed is consistent with an extended matter radius for the ground state of ^{24}O.

We would like to thank the staff of the Coupled Cyclotron Facility at the NSCL for developing and maintaining a high-intensity primary ^{48}Ca beam and the A1900 group for the delivery of the secondary ^{26}F beam. We also would like to thank B. A. Brown, E. Johnson, G. Rogachev, T. Otsuka, K. Tsukiyama, and A. Volya for their enlightening discussions. This work was supported by the National Science Foundation under Grants No. PHY-01-10253, No. PHY-03-54920, No. PHY-04-56463, No. PHY-05-02010, No. PHY-05-55366, No. PHY-05-55445, No. PHY-05-55488 and No. PHY-06-06007.

*calem.hoffman@gmail.com
†Present address: Physics Department, Illinois Wesleyan University, Bloomington, IL 61701, USA.
‡Present address: Department of Physics & Astronomy, Rutgers University, Piscataway, NJ 08854, USA.
§Present address: Department of Physics & Astronomy, Ohio University, Athens, OH 45701, USA.

[1] T. Baumann *et al.*, Nature (London) **449**, 1022 (2007).
[2] D. Guillemaud-Mueller *et al.*, Phys. Rev. C **41**, 937 (1990).
[3] M. Fauerbach *et al.*, Phys. Rev. C **53**, 647 (1996).
[4] O. Tarasov *et al.*, Phys. Lett. B **409**, 64 (1997).
[5] M. Thoennessen *et al.*, Phys. Rev. C **68**, 044318 (2003).
[6] H. Sakurai *et al.*, Phys. Lett. B **448**, 180 (1999).
[7] Y. Utsuno *et al.*, Phys. Rev. C **64**, 011301 (2001).
[8] A. Ozawa *et al.*, Phys. Rev. Lett. **84**, 5493 (2000).
[9] T. Otsuka *et al.*, Phys. Rev. Lett. **87**, 082502 (2001).
[10] T. Otsuka *et al.*, Phys. Rev. Lett. **95**, 232502 (2005).
[11] M. Stanoiu *et al.*, Phys. Rev. C **69**, 034312 (2004).
[12] Z. Elekes *et al.*, Phys. Rev. Lett. **98**, 102502 (2007).
[13] B. A. Brown and B. H. Wildenthal, Annu. Rev. Nucl. Part. Sci. **38**, 29 (1988).
[14] Y. Utsuno *et al.*, Phys. Rev. C **60**, 054315 (1999).
[15] B. A. Brown and W. A. Richter, Phys. Rev. C **74**, 034315 (2006).
[16] P. Möller *et al.*, At. Data Nucl. Data Tables **59**, 185 (1995).
[17] M. Samyn *et al.*, Phys. Rev. C **70**, 044309 (2004).
[18] J. L. Lecouey, Few-Body Syst. **34**, 21 (2004).

[19] D. J. Morrissey *et al.*, Nucl. Instrum. Methods Phys. Res., Sect. B **204**, 90 (2003).
[20] M. D. Bird *et al.*, IEEE Trans. Appl. Supercond. **15**, 1252 (2005).
[21] N. Frank *et al.*, Nucl. Instrum. Methods Phys. Res., Sect. A **580**, 1478 (2007).
[22] T. Baumann *et al.*, Nucl. Instrum. Methods Phys. Res., Sect. A **543**, 517 (2005).
[23] A. Schiller *et al.*, Phys. Rev. Lett. **99**, 112501 (2007).
[24] A. M. Lane and R. G. Thomas, Rev. Mod. Phys. **30**, 257 (1958).
[25] B. Jurado *et al.*, Phys. Lett. B **649**, 43 (2007).
[26] G. Audi *et al.*, Nucl. Phys. **A729**, 3 (2003).
[27] D. Cortina-Gil *et al.*, Phys. Rev. Lett. **93**, 062501 (2004).
[28] C. Nociforo *et al.*, Phys. Lett. B **605**, 79 (2005).
[29] T. Otsuka and K. Tsukiyama (to be published).
[30] A. Ozawa, T. Suzuki, and I. Tanihata, Nucl. Phys. **A693**, 32 (2001).
[31] Z. Ren *et al.*, Phys. Rev. C **52**, R20 (1995).
[32] T. Siiskonen, P. O. Lipas, and J. Rikovska, Phys. Rev. C **60**, 034312 (1999).